




SPECIAL ISSUE ARTICLE

Electric field-assisted sintering anode-supported single solid oxide fuel cell

Reginaldo Muccillo¹  | Daniel Zanetti de Florio²  | Fabio C. Fonseca¹  |
Sabrina G. M. Carvalho¹ | Eliana N. S. Muccillo¹

¹ Energy and Nuclear Research Institute, Cidade Universitária, Sao Paulo, SP, Brazil

² Center for Engineering, Modeling and Applied Social Sciences, Federal University of ABC, Santo André, SP, Brazil

Correspondence

Reginaldo Muccillo, Energy and Nuclear Research Institute, Travessa R 400, Cidade Universitária, Sao Paulo, SP 05508-170, Brazil.

Email: muccillo@usp.br

Funding information

Comissão Nacional de Energia Nuclear-CNEN, Fundação de Amparo à Pesquisa do Estado de São Paulo-FAPESP, Grant/Award Numbers: CINE-SHELL-ANP 2017/11937-4, CEPID-CDMF 2013/07296-2; Conselho Nacional de Desenvolvimento Científico e Tecnológico-CNPq, Grant/Award Numbers: 302357/2018-1, 305889/2018-4, 305620/2019-3

Abstract

Cosintering (La_{0.84}Sr_{0.16}MnO₃ thin-film cathode/ZrO₂: 8 mol% Y₂O₃ thin-film solid electrolyte/55 vol.% ZrO₂:8 mol% Y₂O₃ + 45 vol.% NiO anode, $\phi = 12 \times 1.5$ mm thick pellet) was achieved by applying an electric field for 5 min at 1200°C. Impedance spectroscopy measurements of the anode-supported three-layer cell show an improvement of the electrical conductivity in comparison to that of a conventionally sintered cell. The scanning electron microscopy images of the cross-sections of electric field-assisted pressureless sintered cells show a fairly dense electrolyte and porous anode and cathode. Joule heating, resulting from the electric current due to the application of the AC electric field, is suggested as responsible for sintering. Dilatometric shrinkage curves, electric voltage and current profiles, impedance spectroscopy diagrams, and scanning electron microscopy micrographs show how anode-electrolyte-cathode ceramic cells can be cosintered at temperatures lower than the usually required.

KEYWORDS

anode-supported solid oxide fuel cell, dilatometry, electric field-assisted sintering, impedance spectroscopy

1 | INTRODUCTION

The development of planar unitary solid oxide fuel cells is still under way, in the search for electrically efficient and mechanically reliable single devices, not considering thermo-chemical and thermo-mechanical compatibility when dealing with a stack composite.¹ The manufacture of those devices requires several sintering steps depending on the way their conformation is performed: (a) *one* is sintering the anode to get a porous structure, coating with the electrolyte to be fired to get nonporous electrolyte structure; subsequently, the cathode is deposited on top of the electrolyte, the whole cell being fired again to

get porous cathode structure. However, find the suitable (temperature-heating rate-dwelling time-cooling rate-atmosphere) profile is not an easy task; (b) *another* is single step cofiring the three components (anode, electrolyte, and cathode layers) conformed by tape casting, considered a low-cost SOFC manufacturing technique.^{2–6} Electrolyte sintering is one important step for the cofiring process. The required anode and cathode sintering temperatures for achieving porous structures are lower than the one required for obtaining a dense electrolyte; consequently, after sintering at these low temperatures, the electrolyte would not reach the density required for avoiding fuel permeation at the operation temperature of the whole cell. The use of sintering aid to the electrolyte is one method to lower its sintering temperature.^{7–10} After

Honoring Dr. Mrityunjay Singh

solving the problem of the choice of adequate temperature for cofiring anode and electrolyte, another problem remains to be solved: to find an adequate temperature to cofire the cathode to keep it porous and single phase.^{11,3}

The mismatch of the thermal expansion coefficients of the cell components causes warping and delamination of the cell and may increase porosity of the electrolyte in electrophoretic deposited anode supported cells.¹² During the manufacturing of a cell, thermal stresses are unavoidable due to temperature cycling from room temperature to the firing temperature. In proton conducting half-SOFCs, it has been shown that the driving force for deformation is associated with a porosity gradient, produced during cofiring with a porous load to avoid warping.¹³

Forcing flatness promotes microcracks and porosity in the electrolyte, which could be corrected by additional low viscosity electrolyte coatings followed by additional firings, a tedious and costly solution to the warping problem. A study of the prediction of warping conditions, based on fracture mechanics, has been reported.¹⁴

Besides the warping problem, another difficulty is that during cell operation at temperatures higher than 700°C, the presence of O₂ might oxidize Ni of the Ni-electrolyte anode of the cell, with concentration gradients appearing in the anode layer, leading to electrolyte cracking and warping.¹⁵

Electric field-assisted sintering without application of a mechanical stress on polycrystalline ceramic materials, mainly in electroceramics, has been in the last few years largely reported. Sintering a green ceramic piece can be achieved in a short time (usually few seconds, then the denomination “flash sintering”) with a setup consisting basically of a power supply and a laboratory furnace. This sintering method has been applied, for example, to Y₂O₃-stabilized ZrO₂,^{16–25} MgO-doped Al₂O₃,²⁶ Co₂MnO₄,²⁷ Gd₂O₃-doped BaCeO₃,²⁸ SiC,²⁹ Gd₂O₃-doped CeO₂,³⁰ SrTiO₃,³¹ SnO₂,³² and Y₂O₃,³³ ThO₂,³⁴ and UO₂.³⁵

Anode/electrolyte half SOFCs have already been cosintered by electric field-assisted sintering under pressure (SPS, Spark Plasma Sintering). This technique differs considerably with the flash sintering technique for the following main reasons: a relatively low DC voltage (1–10 V) is applied to a graphite die under vacuum to produce extremely large currents (kA range) resulting in a very large heating rate in a powder specimen under pressure inside the die. This technique requires expensive equipment, while flash sintering could be carried out with a furnace and a programmable power supply. A SPS experiment on a half SOFC allowed for reduction of the NiO with pore former in the anode, crack-free, and well-bonded anode/electrolyte interface and, very important, no warping.³⁶ The flash sintering technique has also been

proposed for manufacturing SOFC components^{16,37} and anode-electrolyte multilayers.³⁸

Attempts for the application of the flash sintering technique to produce single planar three-layer solid oxide fuel cells with porous NiO-YSZ thick anode, dense YSZ thin film, and porous LSM thin film are here reported. The main concern was to produce anode-supported solid oxide fuel cells mechanically stable without microcracks or hot spots to avoid gas permeation.³⁹

2 | MATERIALS AND METHODS

The assembling of the planar anode/electrolyte/cathode three-layer cell consisted of:

1. Anode: 8YSZ/NiO (55/45 vol.%) pressed pellets. 55 vol.% cubic ZrO₂:8 mol% Y₂O₃ (TZ-8Y, Tosoh, Japan) composed of 75 μm spherical granules were thoroughly mixed to 45 vol.% NiO in an agate mortar, uniaxially pressed (50 MPa, Kratos, Brazil) into disc-shaped pellets with 12 mm diameter and approximately 2 mm thickness, followed by isostatic pressing (140 MPa, National Forge Co., USA);
2. Electrolyte: TZ-8Y commercial powder from the same batch used in the anode was diluted in isopropanol; that slurry was brush-painted to one of the anode surfaces. The anode/electrolyte compound was heat treated at 300°C for eliminating the isopropanol. If cracks were produced in the electrolyte, additional layers of the slurry were applied with further 300°C calcinations.
3. Cathode: A (La_{0.80}Sr_{0.20})_{0.95}MnO_{3-x} (lanthanum strontium manganite) paste (LSM, Fuel Cell Materials, USA) was brush-painted on top of the dried electrolyte slurry. The anode/electrolyte/anode compound was again heat treated at 300°C for eliminating organics in the paste. If cracks were produced in the cathode, additional layers of the paste were applied with further 300°C calcinations.

Linear shrinkage was monitored in a pc controlled high-temperature vertical dilatometer (Unitherm 1161V, Pittsburgh, USA) with platinum grids on both parallel sides of the sample. Platinum wires connected these current collectors either to a custom-made power supply (0–55 V, 0–6 A, 0.5–1.2 kHz), or to a Hewlett Packard 4192A impedance analyzer with a 362 HP controller. The $[-Z''(\omega) \times Z'(\omega)]$ impedance spectroscopy data were obtained in the 5 Hz–13 MHz frequency range [$f = (\omega/2\pi)$] under a voltage amplitude of 200 mV and at temperatures within the oxide ion conductivity region. All experiments were performed at ambient atmosphere. Further details may be found elsewhere.²²

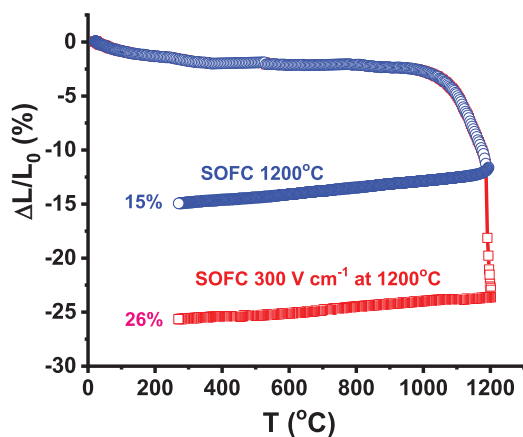


FIGURE 1 Dilatometric curves of anode-supported planar three-layer cell from RT to 1200°C without and with application of 310 V/cm, 1 kHz, 1 A, for 5 min at 1200°C

The isothermal flash sintering experiment consisted in heating the three-layer cell and applying an AC voltage (AC for only charge transport, DC could transport undesirable mass)^{40,41} when the specimen reached a pre-established temperature. The shrinkage level was monitored at the dilatometer gauge while the electrical data (applied voltage and the current through the cell) were collected with digital voltmeters connected to a computer.²² Typical value of applied voltage was 50 V in 1.6 mm sample thickness (310 V/cm), limiting the electric current to 1 A (0.88 A/cm²).

Fracture cross-section surfaces of the sintered cells were observed in a Inspect F50 FEG-SEM (FEI, Brno, Czech Republic) scanning electron microscope with EDS (EDAX) analysis, applying 20 kV accelerating voltage with 3.0 spot size. No special preparation, like polishing and/or etching of the cell surfaces, was done.

3 | RESULTS

3.1 | Sintering: Conventional and electric field-assisted

Figure 1 shows two linear shrinkage curves of a single three-layer cell, one upon heating at 10°C/min to 1200°C, and other applying 310 V/cm, 1 kHz, 1 A limiting current, for 5 min when the sample reached 1200°C. The contribution of the electric field is evident with 11% improvement in the shrinkage of the whole cell.

Figure 2 shows the applied electric voltage and current during the flash sintering experiment. The power supply gives the appropriate voltage amplitude such as to keep the limiting current value, 1 A in this case. The incubation time, that is, the elapsed time the flash event takes

place after the application of the electric voltage, is approximately 70 s.

3.2 | SEM analysis

The cross-section of the planar three-layer cell flash-sintered at 1200°C was observed in the FEG scanning electron microscope. The micrograph of a typical region is shown in Figure 3.

Figure 4 shows the mapping of the elements in a line profile from the inner part of the anode to the cathode extremity of the cell (left to right). Zirconium, yttrium, and nickel were found at the anode, zirconium, and yttrium at the electrolyte, as expected.

Figure 5 shows scanning electron microscopy micrographs of anode, electrolyte, and cathode along with the corresponding EDS analysis.

3.3 | Impedance spectroscopy analysis

Impedance spectroscopy data of the three-layer cell flash-sintered at 1200°C during 5 min with 310 V/cm, 1k Hz, with 1 A limiting current, were collected at 590°C from 5 Hz to 13 MHz, input signal 200 mV. The $[-Z''(\omega) \times Z'(\omega)]$ impedance diagrams are shown in Figure 6.

4 | DISCUSSION

4.1 | Sintering: Conventional and electric field-assisted

Figure 1 shows that heating the cell to 1200°C promotes (from the anode to the cathode) a cross-section shrinkage of 15% of the cell thickness without the application of the electric field, while under the applied electric field the shrinkage reached 26%. We must point out that approximately 26% is the threshold level for 8YSZ reaching full density at 1450°C.^{42,43} This is the evidence of the possibility of cosintering a single solid oxide fuel cell at furnace temperatures lower than the usual, by applying an electric field. Care should be taken for appropriate choice of the electric voltage, the exposure time, and the limitation of the electric current through the sample. Excessive current or exposure time could provide too much Joule heating, resulting in disruption of the sample.³⁹

4.2 | SEM analysis

The electron microscopy analysis of the cross-section of the flash sintered cell, Figure 3, shows a porous cathode and all cell components well welded, 13 μm being the

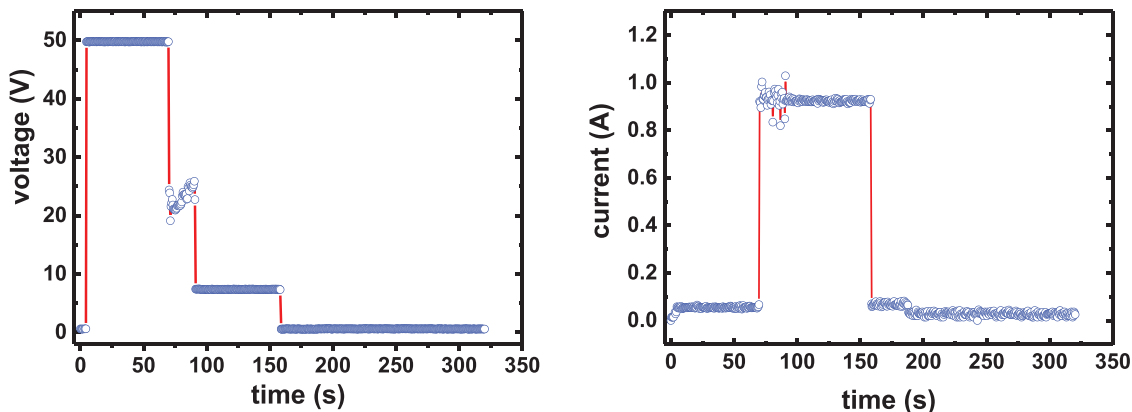


FIGURE 2 Typical applied electric voltage (50 V) and current (1 A) through the anode-electrolyte-cathode cell during the flash sintering experiment

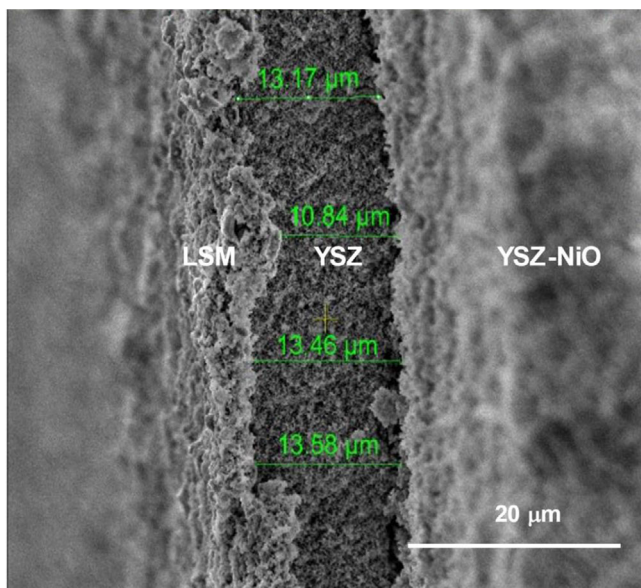


FIGURE 3 Scanning electron microscopy image of a cross-section of a planar unitary three-layer cell after flash sintering with 310 V/cm, 1 kHz, 1 A, for 5 min at 1200°C. LSM: Lanthanum Strontium Manganite cathode; YSZ: 8 mol% yttria-stabilized zirconia solid electrolyte; YSZ + NiO: anode

approximate average thickness of the dense 8YSZ solid electrolyte. The flash sintering at 1200°C did sinter the three components of the planar three-layer cell, with grain-to-grain neck formation. The EDS analysis on the anode and cathode shows Ni in the former and Mn, La, and Sr in the latter. Zr is detected due to the limitation in the spot size of the scanning electron microscope. Anode and cathode are porous as required for percolation of the fuel and the oxidant. The electrolyte is fairly dense, its porous region concentrated on its outer surface. The elemental analysis shows the occurrence of La and Mn from the cathode.

Line scanning of the elements across the section of the cell, Figure 4, shows Zr, Y, and Ni in the relatively thick

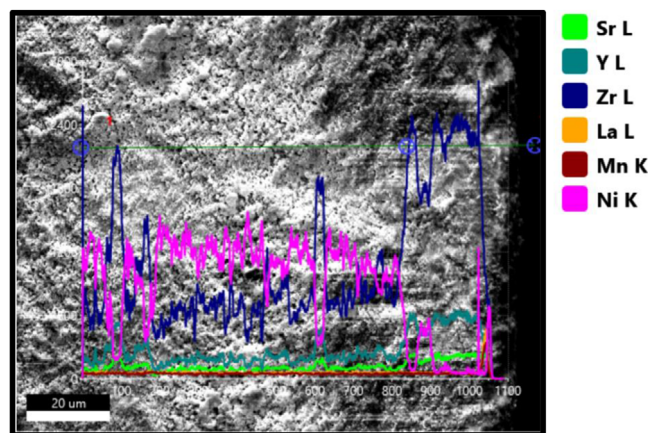


FIGURE 4 Scanning electron microscopy energy-dispersive X-ray line scanning of Zr, Y, Ni, La, Sr, Mn elements across the cross-section of the single planar three-layer cell flash sintered with 310 V/cm, 1 kHz, 1 A, for 5 min at 1200°C

anode. It was difficult to detect La, Sr, and Mn in the cathode side due to limitation of the detection technique and its thin-film structure.

Figure 5 depicts the scanning electron microscopy micrographs of anode, electrolyte, and cathode along with the corresponding EDS analysis. Higher magnification shows welded grains in the three components, evidencing the high temperature reached by the cell during flash sintering.

4.3 | Impedance spectroscopy analysis

The impedance spectroscopy diagrams shown in Figure 6 for the cell sintered at 1200°C with and without the application of an electric field consist of broad decentralized semicircles, resulting from the contribution of the bulk (intragranular, grains) and of the interfaces (intergranular,

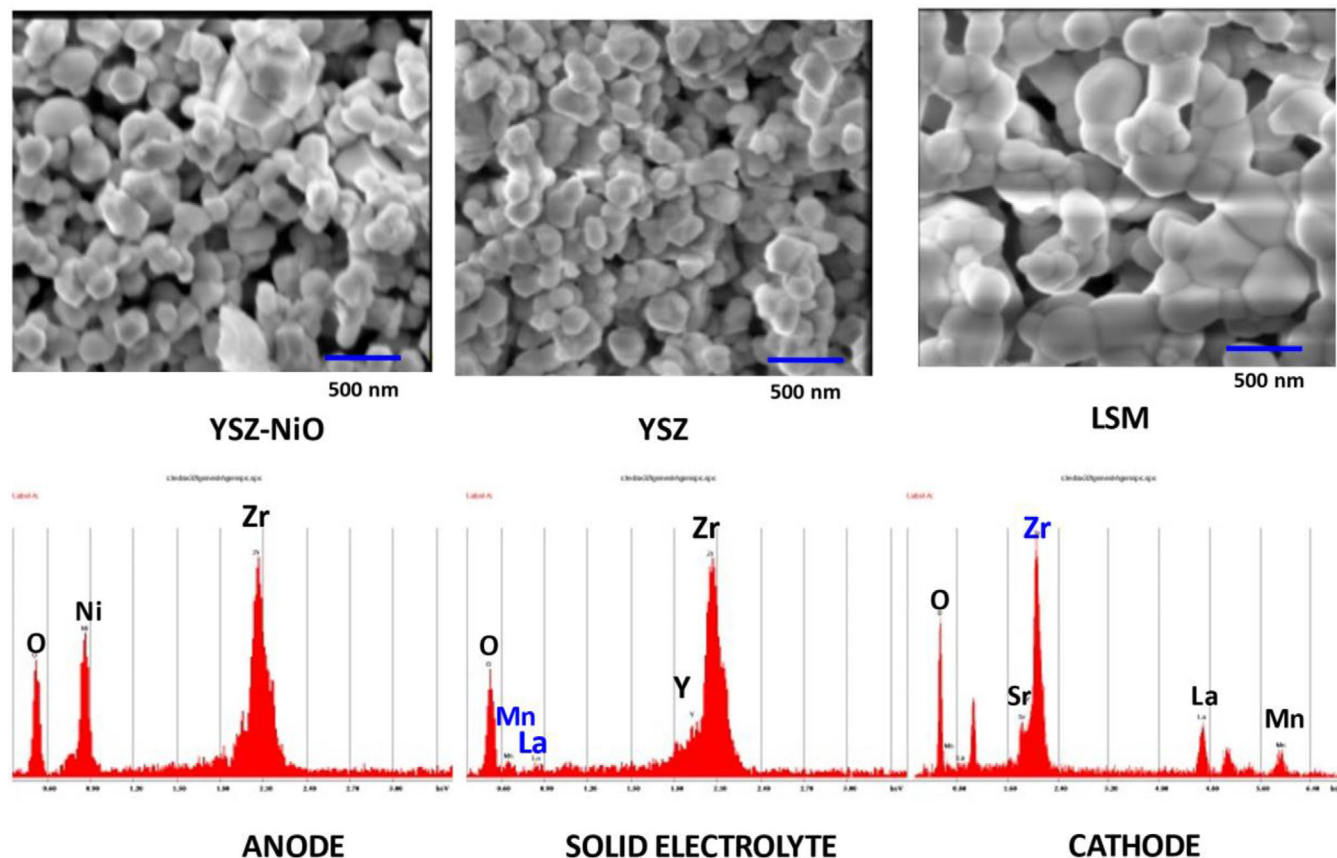


FIGURE 5 Scanning electron microscopy images of the components of a planar three-layer cell after flash sintering with 310 V/cm, 1 kHz, 1 A, for 5 min at 1200°C. YSZ-NiO: anode; YSZ: 8 mol% yttria-stabilized zirconia solid electrolyte; LSM: Lanthanum Strontium Manganite cathode. Bottom: Results of EDS analysis

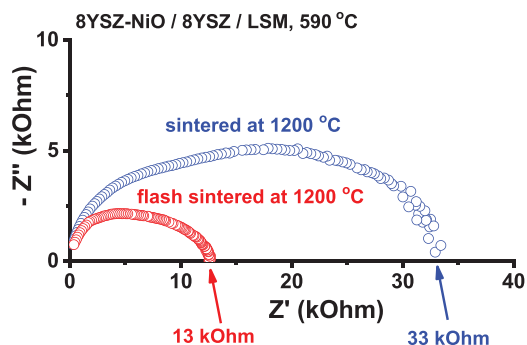


FIGURE 6 Impedance diagrams of planar three-layer cells after flash sintering with 310 V/cm, 1 kHz, 1 A, for 5 min at 1200°C and after cosintering at 1200°C (conventional). Input signal 200 mV; frequency range 5 Hz-13 MHz; temperature of measurement 590°C. Blue and red: experimental data

grain boundaries, and pores).^{42,44} The total electrical resistance of the conventionally sintered cell, measured at the intersection of the impedance diagram with the Z' axis at the low frequency side of the diagram, is 33 kOhm. The flash sintered cell, on the other hand, after 5 min of 1 A electric current applied at 1 kHz, had its total electric resis-

tance reduced to 13 kOhm. Under operational conditions, this value would be lower after nickel oxide reduction to nickel by the fuel atmosphere, usually hydrogen.⁴⁵

Improvement of the ionic conductivity of 8YSZ had already been reported.^{22–25} The major contribution to the electrical resistance of the cell might be due to the thicker anode. The reduction of the electrical resistance in the flash sintered cell is tentatively ascribed to additional heating produced in the bulk of the cell by the flow of the electric current (Joule heating).

5 | CONCLUSIONS

Single anode-supported solid oxide fuel cells prepared by coating an anode composed of 8 mol% yttria-stabilized zirconia and nickel oxide (55/45 vol.%) with an 8 mol% yttria-stabilized zirconia film and, on top of that, a film of lanthanum strontium manganite, were cosintered at 1200°C and also at that same temperature applying 310 V/cm AC voltage during 5 min. The stepwise application of AC electric voltages to the cell promoted an enhancement of the shrinkage level from 15 to 26%. Moreover, the scanning

electron microscopy images showed that the microstructures of the flash sintered cells present suitable densification with porous both anode and cathode, and fairly dense electrolyte. The densification promoted by flash sintering leads also to a 63% decrease in the total electric resistivity of the cell. Joule heating is proposed as the main mechanism responsible for the densification of the planar three-layer cell.

ACKNOWLEDGMENTS

To Francisco N. Tabuti and Yone V. França for technical support. S.G.M.C. holds a Post-doctoral fellowship provided by Shell.

FUNDING

This work was supported by Comissão Nacional de Energia Nuclear-CNEN, Fundação de Amparo à Pesquisa do Estado de São Paulo-FAPESP (CINE-SHELL-ANP 2017/11937-4 and CEPID-CDMF 2013/07296-2), and Conselho Nacional de Desenvolvimento Científico e Tecnológico-CNPq (302357/2018-1, 305889/2018-4, and 305620/2019-3).

CONFLICT OF INTEREST

The authors state that there is no conflict of interest.

AUTHOR'S CONTRIBUTION

Statement of contribution for each author: R. Muccillo (leader, advisor: design, experimentation, analysis, writing, approval); D.Z. de Florio (contributor: experimentation, analysis, writing); F.C. Fonseca (contributor: experimentation, analysis, writing); S.G.M. Carvalho (contributor: experimentation); E.N.S. Muccillo (contributor: experimentation, analysis, writing).

ORCID

Reginaldo Muccillo  <https://orcid.org/0000-0002-8598-279X>

Daniel Zanetti de Florio  <https://orcid.org/0000-0002-7291-1917>

Fabio C. Fonseca  <https://orcid.org/0000-0003-0708-2021>

REFERENCES

1. Yamamoto O. Solid oxide fuel cells: Fundamental aspects and prospects. *Electrochim Acta*. 2000;45:2423-35.
2. Jae-ha M, Tae ho S, Sun-Dong K, Hae-Gu P, Moon J, Moon SH. Optimization of Ni-zirconia based anode support for robust and high-performance 5 x 5 cm² sized SOFC via tape-casting/co-firing technique and nano-structured anode. *Int J Hydrogen Energy*. 2015;40:2792-9.
3. Moon H, Kim SD, Hyun SH, Kim HS. Development of ITSOFC unit cells with anode-supported thin electrolytes via tape casting and co-firing. *Int J Hydrogen Energy*. 2008;33:1758-68.
4. Moon H, Kim SD, Park EW, Hyun SH, Kim HS. Characteristics of SOFC single cells with anode active layer via tape casting and co-firing. *Int J Hydrogen Energy*. 2008;33:2826-33.
5. Myung JH, Ko HJ, Park HG, Hwan M, Hyun SH. Fabrication and characterization of planar-type SOFC unit cells using the tape-casting/lamination/co-firing method. *Int J Hydrogen Energy*. 2012;37:498-504.
6. Ye G, Ju F, Lin C, Gopalan S, Pal U, Seccombe D. Single-step co-firing technique for SOFC fabrication. *ECS Trans*. 2005;8:451-9.
7. Fagg DP, Abrantes JCC, Pérez-Coll D, Nuñez P, Kharton VV, Frade JR. The effect of cobalt oxide sintering aid on electronic transport in Ce_{0.80}Gd_{0.20}O_{2-d} electrolyte. *Electrochim Acta*. 2003;48:1023-9.
8. Zhang TS, Ma J, Leng YJ, Chan SH, Hing P, Kilner JA. Effect of transition metal oxides on densification and electrical properties of Si-containing Ce_{0.8}Gd_{0.2}O_{2-d} ceramics. *Solid State Ionics*. 2004;168:187-95.
9. Kleinogel C, Gauckler LJ. Sintering of nanocrystalline CoO₂ ceramics. *Adv Mater*. 2001;13:1081-5.
10. Horovistiz AL, Muccillo ENS. Microstructural and electrical characterization of chemically prepared Ce_{0.8}Gd_{2-x}(Ag,Sr)_xO_{1.9} (0 ≤ x ≤ 0.02). *Solid State Ionics*. 2012;225:428-31.
11. Song HS, Kim WK, Hyun SH, Moon J, Kim J, Lee H-W. Effect of starting particulate materials on microstructure and cathodic performance of nanoporous LSMeYSZ composite cathodes. *J Power Sources*. 2007;167:258-64.
12. Lankin MK, Karan K. Effect of processing conditions on curvature of anode/electrolyte SOFC half-cells fabricated by electrophoretic deposition. *J Fuel Cell Sci Technol*. 2009;6:021001-8.
13. Costa R, Hafsaoui J, Oliveira APA, Grosjean A, Caruel M, Chesnaud A, Thorel A. Tape casting of proton conducting ceramic material. *J Appl Electrochem*. 2009;39:485-95.
14. Liu WN, Sun X, Khaleel MA, Qu JM. Global failure criteria for positive/electrolyte/negative structure of planar solid oxide fuel cell. *J Power Sources*. 2009;192:486-93.
15. Young JL, Birss VI. Crack severity in relation to non-homogeneous Ni oxidation in anode-supported solid oxide fuel cells. *J Power Sources*. 2011;196:7126-35.
16. Cologne M, Prette ALG, Raj R. Flash-sintering of cubic yttria-stabilized zirconia at 750°C for possible use in SOFC manufacturing. *J Am Ceram Soc*. 2011;94:316-9.
17. Muccillo R, Kleitz M, Muccillo ENS. Flash grain welding in yttria stabilized zirconia. *J Eur Ceram Soc*. 2011;31:1517-21.
18. Cordier A, Kleitz M, Steil MC. Welding of yttrium-doped zirconia granules by electric current activated sintering (ECAS): Proton formation as a possible intermediate step in the consolidation mechanism. *J Eur Ceram Soc*. 2012;32:1473-9.
19. Downs JA, Sglavo VM. Electric field assisted sintering of cubic zirconia at 390°C. *J Am Ceram Soc*. 2013;96:1342-4.
20. Baraki R, Schwarz S, Guillon O. Effect of electrical field/current on sintering of fully stabilized zirconia. *J Am Ceram Soc*. 2012;95:75-8.
21. Steil MC, Marinha D, Aman Y, Gomes JRC, Kleitz M. From conventional AC flash-sintering of YSZ to hyper-flash and double-flash. *J Eur Ceram Soc*. 2013;33:2093-101.

22. Muccillo R, Muccillo ENS. An experimental setup for shrinkage evaluation during electric field-assisted flash sintering: Application to yttria-stabilized zirconia. *J Eur Ceram Soc.* 2013;33:515-20.
23. M'Peko J-C, Francis JSC, Raj R. Impedance spectroscopy and dielectric properties of flash versus conventionally sintered yttria-doped zirconia electroceramics viewed at the microstructural level. *J Am Ceram Soc.* 2013;96:3760-7.
24. Adam YD, Stevenson AJ, Vernat D, Diaz M, Marinha D. Estimating Joule heating and ionic conductivity during flash sintering of 8YSZ. *J Eur Ceram Soc.* 2016;36:749-59.
25. Vendrell X, Yadav D, Raj R, West AR. Influence of flash sintering on the ionic conductivity of 8 mol% yttria stabilized zirconia. *J Eur Ceram Soc.* 2019;39:1252-8.
26. Cologna M, Francis JSC, Raj R. Field assisted and flash sintering of alumina and its relationship to conductivity and MgO-doping. *J Eur Ceram Soc.* 2011;31:2827-37.
27. Prette ALG, Cologna M, Sglavo V, Raj R. Flash sintering of Co_2MnO_4 spinel for solid oxide fuel cell applications. *J Power Sources.* 2011;196:2061-5.
28. Muccillo R, Muccillo ENS, Kleitz M. Densification and enhancement of grain boundary conductivity of gadolinium-doped barium cerate by ultra fast flash grain welding. *J Eur Ceram Soc.* 2012;33:2311-6.
29. Zapata-Solvas E, Bonilla S, Wilshaw PR, Todd RI. Preliminary investigation of flash sintering of SiC. *J Eur Ceram Soc.* 2013;33:2811-6.
30. Hao X, Liu Y, Wang Z, Qiao J, Sun K. A novel sintering method to obtain fully dense gadolinia doped ceria by applying a direct current. *J. Power Sources.* 2012;210:86-91.
31. Karakuscu A, Cologna M, Yarotski D, Won J, Francis JSC, Raj R, Uberuaga BP. Defect structure of flash-sintered strontium titanate. *J Am Ceram Soc.* 2012;95: 2531-6.
32. Muccillo R, Muccillo ENS. Electric field-assisted flash sintering of tin dioxide. *J Eur Ceram Soc.* 2014;34:915-23.
33. Yoshida H, Sakka Y, Yamamoto T, Lebrun J-M, Raj R. Densification behavior and microstructural development in undoped yttria prepared by flash sintering. *J Eur Ceram Soc.* 2014;34:991-1000.
34. Straka W, Amoah S, Schwartz J. Densification of thoria through flash sintering. *MRS Comm.* 2017;7:677-82.
35. Raftery AM, da Silva JGP, Byler DD, Andersson DA, Uberuaga BP, Stanek CR, McClellan KJ. Onset conditions for flash sintering of UO_2 . *J Nuclear Mater.* 2017;493:264-70.
36. Bezdorozhev O, Borodianska H, Sakka Y, Vasylykiv O. Spark plasma sintered Ni-YSZ/YSZ by-layers for solid oxide fuel cell. *J Nanosci Nanotechnol.* 2013;13:4150-7.
37. Liu Y, Hao X, Wang Z, Wang J, Qiao J, Sun K. A newly developed effective current assisted sintering technique for electrolyte film densification of anode-supported solid oxide fuel cells. *J Power Sources.* 2012;215:296-300.
38. Francis JSC, Cologna M, Montinaro D, Raj R. Flash sintering of anode-electrolyte multilayers for SOFC applications. *J Am Ceram Soc.* 2013;96:1352-4.
39. Jones GM, Biesuz M, Ji W, John SF, Grimley C, Manière C, Dance CEJ. Promoting microstructural homogeneity during flash sintering of ceramics through thermal management. *MRS Bull.* 2021;46:59-66.
40. Conrad H, Yang D. Effect of the strength of an AC electric field compared to DC on the sintering rate and related grain size of zirconia (3Y-TZP). *Mater Sci Eng A.* 2013;559:591-4.
41. Grimley CA, Prette ALG, Dickey EC. Effect of boundary conditions on reduction during early stage flash sintering of YSZ. *Acta Mater.* 2019;174:271-8.
42. Steil MC, Thévenot F, Kleitz M. Densification of yttria stabilized zirconia. *J Electrochem Soc.* 1997;144:390-8.
43. Muccillo RM, Muccillo E. Shrinkage control of yttria-stabilized zirconia during AC electric field-assisted sintering. *J Eur Ceram Soc.* 2014;34:3871-7.
44. Kleitz M, Bernard H, Fernandez E, Schouler E. Impedance spectroscopy and electrical resistance measurements on stabilized zirconia. In Heuer AH, Hobbs LW, editors. *Advances in ceramics, Vol. 3, Science and technology of zirconia.* Columbus, OH: Am Ceram Soc, Inc, 1981; p. 310.
45. Menzler NH, Tietz F, Uhlenbruck S, Buchkremer HP, Stöver D. Materials and manufacturing technologies for solid oxide fuel cells. *J Mater Sci.* 2010;45:3109-35.

How to cite this article: Muccillo R, de Florio DZ, Fonseca FC, Carvalho SGM, Muccillo ENS. Electric field-assisted sintering anode-supported single solid oxide fuel cell. *Int J Appl Ceram Technol.* 2022;19:906-912.
<https://doi.org/10.1111/ijac.13871>